Supporting Information

Transparent Tantalum Clusters-based UV and IR Blocking Electro-chromic Devices

A. Renaud,*[a] M. Wilmet,[ab] T. G. Truong,[a] M. Seze,[a] P. Lemoine,[a] N. Dumait,[a]W. Chen,[bc] N. Saito,[be] T. Ohsawa,[de] T. Uchikoshi,[bc] N. Ohashi,[bde] S. Cordier*[a] and F. Grasset*[bd]

[a] Université de Rennes 1, UMR Institut des Sciences Chimiques de Rennes UR1-CNRS 6226, Equipe Chimie du Solide et Matériaux, 263 av. du Général Leclerc, 35042 Rennes, France.
[b]CNRS-SaintGobain-NIMS, UMI 3629, Laboratory for Innovative Key Materials and Structures (LINK),National Institute of Material Science, 1-1 Namiki, Tsukuba 305-0044, Japan.
[c]Fine Particles Engineering Group, RCFM, National Institute of Material Science, 1-2-1 Sengen, Tsukuba, Japan.
[d]NIMS-Saint-Gobain Center of Excellence for Advanced Materials, National Institute of Material Science, 1-1 Namiki, Tsukuba, Ibaraki 305-0044, Japan.
[e] RCFM, National Institute for Materials Science, 1-1 Namiki, Tsukuba, Ibaraki 305-0044, Japan.

* Email: adele.renaud@hotmail.fr; stephane.cordier@univ-rennes1.fr; fabien.grasset@univ-rennes1.fr, grasset.fabien@nims.go.jp

XPS analysis. $K_4Ta_6Br_{18}$ powder wasanalysed by X-ray photoelectron spectroscopy (XPS) technique after deposition on a carbon tape. It was performed on aSigmaProbe (Thermo Fisher Scientific) spectrometer, equipped with the excitation source of Al-Kα line (1486 eV). Data treatments were carried out using the software ThermoAvantage and the spectra energy was calibrated with the first deconvolvedC 1s peak (attributed to the C-C bonding) rescale at 285 eV.

All the peaks of the wide range survey spectrum (Figure S1) can be attributed to the different elements constituting $K_4Ta_6Br_{18}$ powder and carbon and oxygen contamination.

The Br 3p peaks were deconvoluated in two contributions too (189.13 and 187.83 eV for $3p_{1/2}$ peak and 182.81 and 181.10 eV for $3p_{3/2}$ peak) which corresponds to two environments of the inner bromines or apical bromines (Figure S2b and Table S1). Indeed, the area ratio of 3p contributions of the two Br (i. e. $(3p_{1/2}(Br1) + 3p_{3/2}(Br1))/(3p_{1/2}(Br2) + 3p_{3/2}(Br2)) = 1.97 \approx 2$) is in full agreement with the theoretical ratio $Br^i/Br^a = 12/6 = 2$.

The Ta $4f_{5/2}$ and $4f_{7/2}$peaks can be deconvoluatedin two contributions respectively (28.79 and 25.98 eV for $4f_{5/2}$ peak and 26.96 and 24.13 eV for $4f_{7/2}$ peak) which indicates two types of Ta in the compound (Figure S2a and Table S1).As already described in the literature,[S1] we can

attribute the peaks at 25.98 and 24.13 eV to the Ta_6 cluster whereas the second contribution can beexplained by tantalum in oxygen environment comparable to that in Ta_2O_5 compound.[S2]Since no other phase is observed by XRD, TEM or Raman techniques, we assume that this is due to a surface oxidation of the powder. Note that insoluble impurities were removed from $K_4Ta_6Br_{18}$ by dissolution and filtration before integration in PVP.

Thus, all of these results confirm the presence of $K_4Ta_6Br_{18}$compound based on octahedral $[Ta_6Br^i_{12}Br^a_6]$ cluster units.

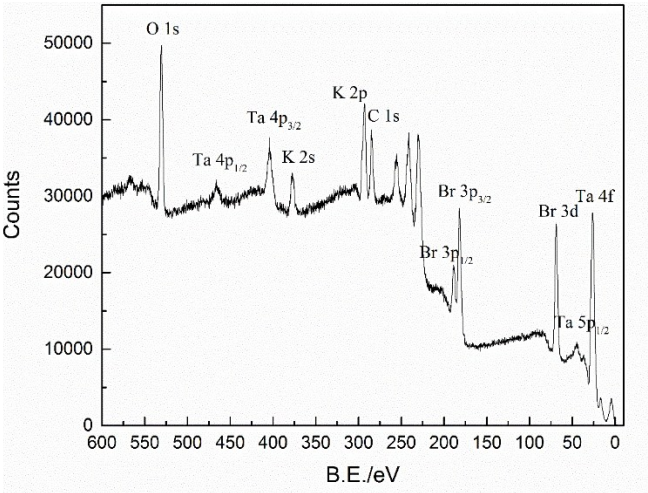

Fig. S1. Wide range survey XPS spectra of $K_4Ta_6Br_{18}$ powder deposited on carbon tape.

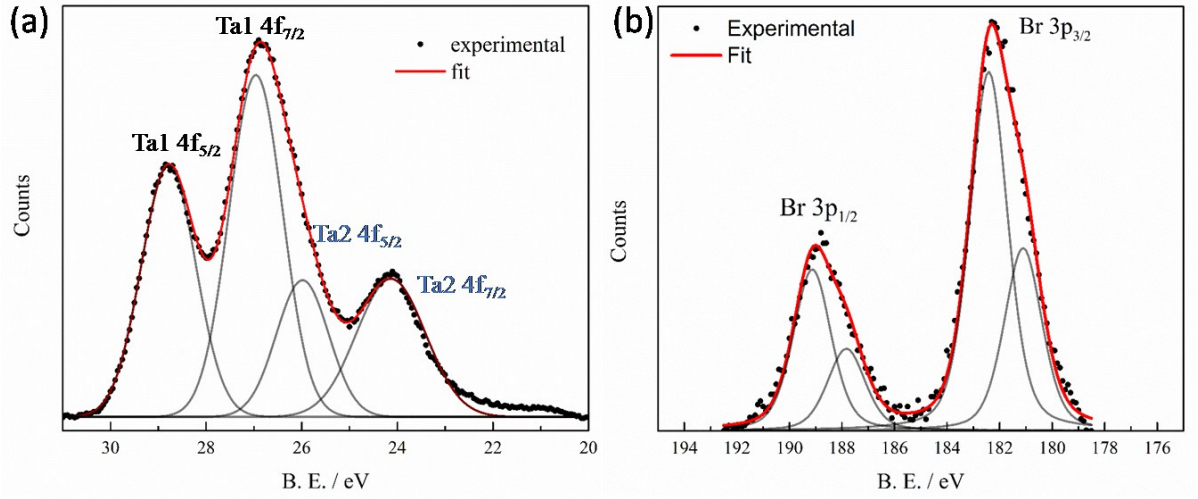

Fig. S2.XPS spectra of (a) Ta 4f and (b) Br 3p of $K_4Ta_6Br_{18}$ powder.

Table S1. Contributions of Ta 4f and Br 3p of $K_4Ta_6Br_{18}$ sample.

	Ta $4f_{5/2}$		Ta $4f_{7/2}$		Br $3p_{1/2}$		Br $3p_{3/2}$	
	Ta1	Ta2	Ta1	Ta2	Br1	Br2	Br1	Br2
B. E./eV	28.79	25.98	26.96	24.13	189.13	187.83	182.41	181.10
FWHM/eV	1.34	1.29	1.32	1.70	1.70	1.70	1.70	1.70
Intensity	1310	684	1747	912	643	327	1429	727

HAADF-STEM observations. Scanning transmission electron microscopy (STEM)images were taken using a Cs-corrected JEOL JEM2100F microscopeoperating at 200 kV. It is equipped with a field-emissionelectron gun and incorporates multiple additional functionssuch as an energy-dispersive spectrometry (EDS) and a highsensitivityZ-contrast high angular annular dark field scanningtransmission electron microscopy (HAADF-STEM) analysis.A sample was prepared by direct deposition of powder (scratch from thin film) on carbon-activated copper grids.The preparation of perfect sample by focused ion beam andultramicrotomy is too much expensive and time-consuming, nevertheless thanks to theHAADF-STEM mode image in high resolution (FigureS3), it is clearly possible to observe the Ta_6 clusters inside the PVP matrix. As it can be observed, the cluster units, represented by light spots, are relatively well dispersed inside the PVP matrix. Ta and Br elements have been clearly detected by EDS and are well distributed in the PVP matrix (Figure S4). Nevertheless,this technique is not accurateto give a chemical composition due to a too high dilution ofthese elements in PVP matrix and a very low stability of the sample under e-beamirradiation.

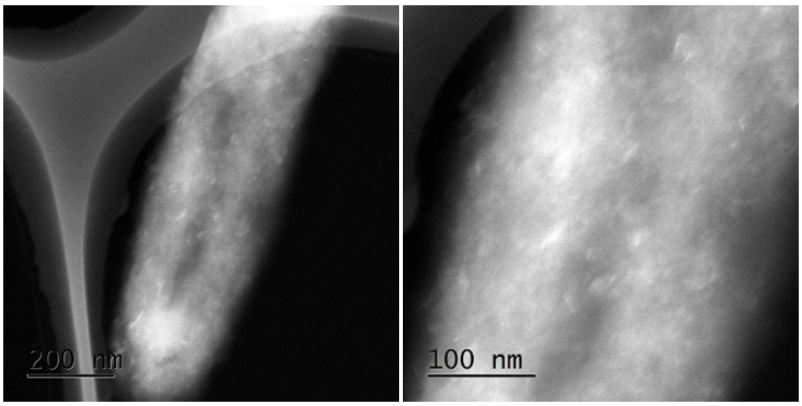

Fig. S3. STEM images of a Ta_6@PVP thin film at different magnifications.

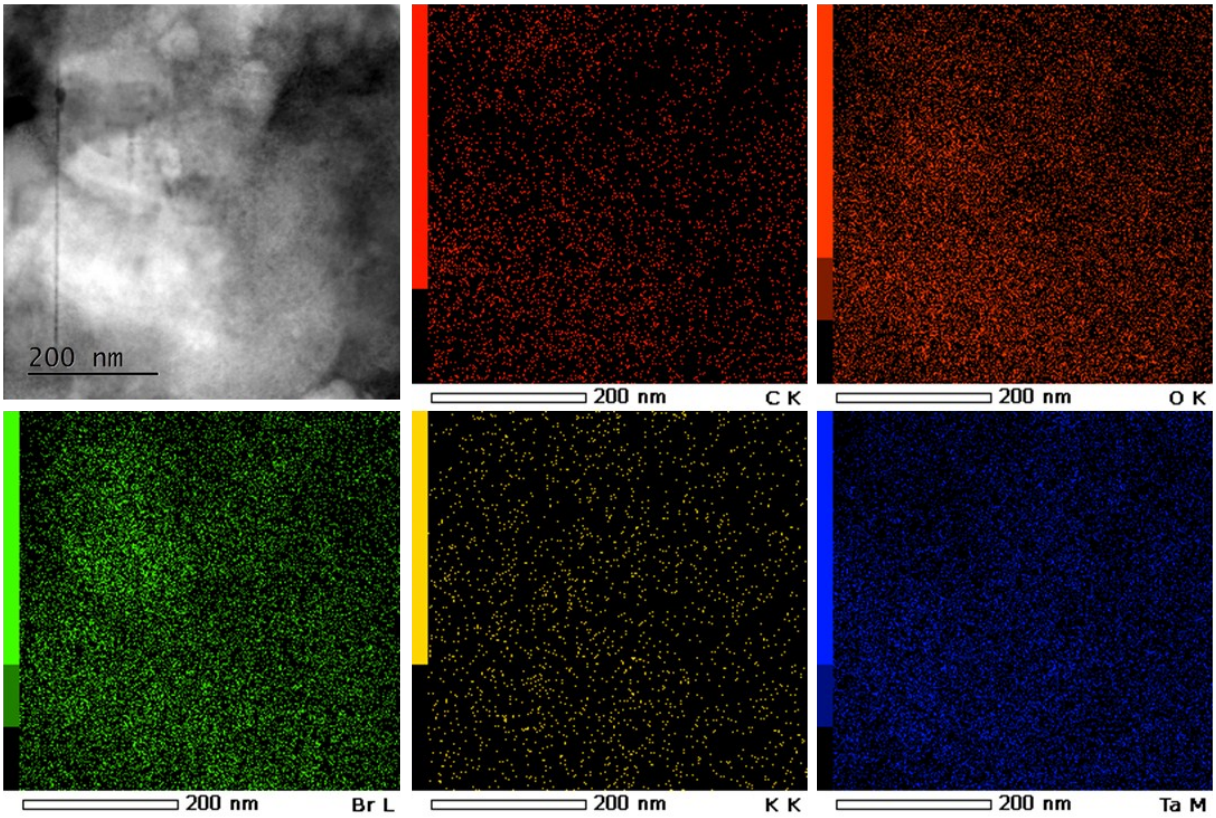

Fig. S4. STEM analysis of Ta_6@PVP thin film.

Raman spectroscopy. Raman scattering spectra of $K_4Ta_6Br_{18}$powderand $K_4Ta_6Br_{18}$@PVPdeposited on glass substrate were measured using a LabRamHigh Resolution spectrometer coupled with a confocal microscope(Horiba YobinYvon), 600 g/mm gratingand 10 × objective. A He-Ne 633 nm laser was usedfor scattering excitation. Raman spectra were recorded at room temperature with 100 s exposition and 2 accumulations. In order to probe the homogeneity of the sample coated on glass, point by point spectra on 5×5 μm^2 areas were recorded using a step of 1 cm. Each point spectra was recorded with 1 s exposition and 2 accumulations. Spectra were average for eachof the four measured area.

Raman spectra of $K_4Ta_6Br_{18}$@PVP deposited on a glass was first recorded and compared with data reported by Preetzet al.[S3] for $Ta_6Br^i_{12}Br^a_{2\text{-}8}H_2O$.These authors made the normal mode determination and conclude that there exist 11 possible basic vibrations considering an O_h symmetry. However, only 4 signals were observed for $Ta_6Br^i_{12}Br^a_{2\text{-}8}H_2O$.Characteristic frequencies of the $M_6X^i_{12}X^a_6$ cluster unitsin $Ta_6Br^i_{12}Br^a_{2\text{-}8}H_2O$are: the symmetric metal-metal vibrationlocated around 176-179 cm^{-1} (ν_1); the Ta-Br^i vibration at 229 cm^{-1} (ν_2) and two Ta_6-Braphase-vibrations(ν_5: 125 cm^{-1}; ν_{12}: 103cm^{-1}). It turns out that experimental spectrum of $K_4Ta_6Br_{18}$@PVP deposited on glass exhibits similar characteristicswith four main bands at ν_{12}

= 99cm^{-1}; ν_5 = 119cm^{-1}; ν_1 = 170cm^{-1}; ν_2 = 225cm^{-1} (Figure S5).These bands compare well with spectra reported by Preetzet al. on $Ta_6Br^i_{12}Br^a_{2-8}H_2O$.On the other hand, one new band with lower intensity appears at 288 cm^{-1}. In order to know more about the origin of this band, the Raman spectrum of $K_4Ta_6Br_{18}$ starting compound was recorded (Figure S6).The latter is characterized by 6 bands:ν_{12} = 99 cm^{-1}; ν_5 = 113cm^{-1}; ν_1 = 165cm^{-1};ν_2 = 226cm^{-1} and two other bands at 129 cm^{-1} and 278 cm^{-1}. Thus, these new bands are assumed to originate from local perturbation of potassium cation around the clusterunits.From $K_4Ta_6Br_{18}$ starting compound to$K_4Ta_6Br_{18}$@PVP deposited on a glass, ν_2 and ν_{12} are almost unchanged, ν_5 shifts from 113 to 119 cm^{-1}, ν_1 from 165 cm^{-1}to 170cm^{-1}.The signal at 278 cm^{-1}is shifted to 288 cm^{-1} whilst the signal at 129 cm-1 almost disappears.The shifts of the bands between starting compounds and coated materials mean that in $K_4Ta_6Br_{18}$@PVP, there exist significant interactions between the $[Ta_6Br^i_{12}Br^a_6]^{4-}$cluster units and the PVP matrix. Moreover, it also demonstrates that in $K_4Ta_6Br_{18}$@PVP, potassium cations are still around the cluster unit. Average spectra of 5×5 cm^2 areas (Figure S7) reveal that the composition of the films is homogeneous revealing a very good dispersion of the clusters within the matrix.

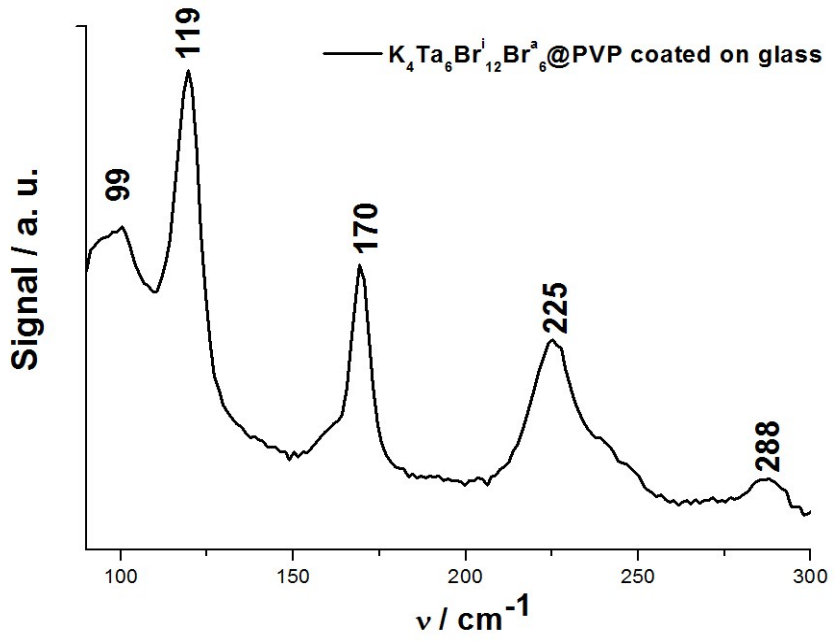

Fig. S5. Raman spectrum of $K_4Ta_6Br_{18}$@PVP recorded for 100 s of exposition and 2 accumulations.

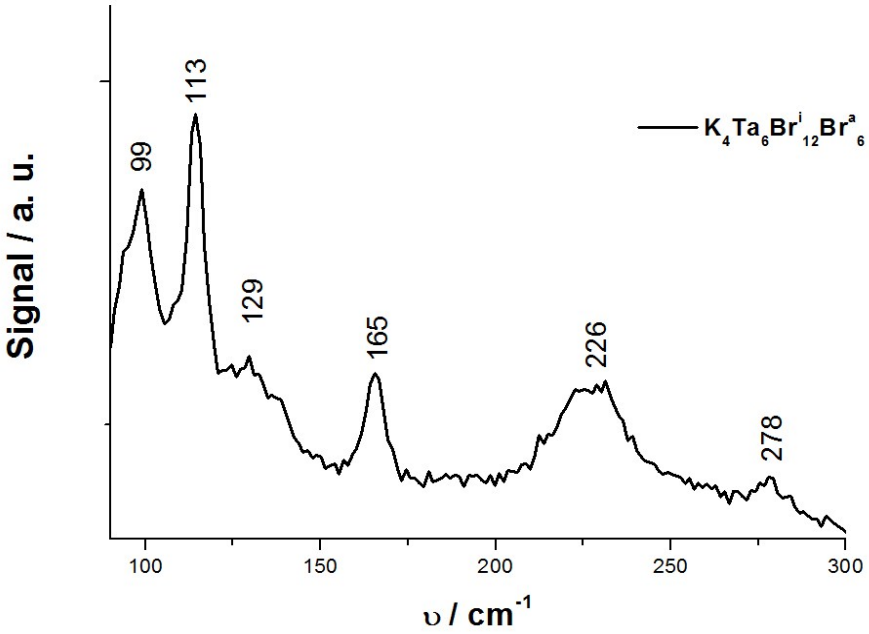

Fig. S6. Raman spectrum of $K_4Ta_6Br_{18}$powder recorded for 100 s of exposition and 2 accumulations.

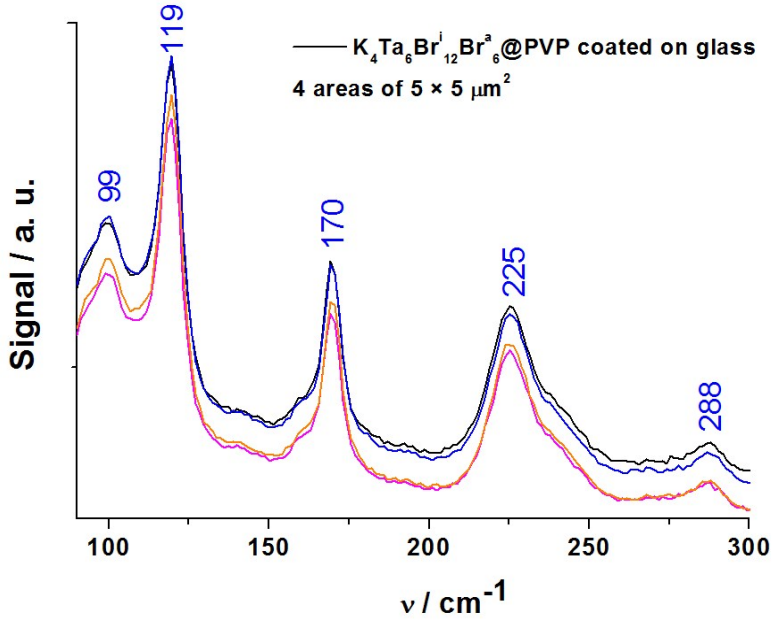

Fig. S7. Average Raman spectra of 4 selected 5×5 cm^2areas of $K_4Ta_6Br_{18}$@PVP.

Xray diffraction experiments.

X-ray powder diffraction (XRPD) data of the $K_4Ta_6Br_{18}$starting powder were collected at room temperature using a Bruker D8 Advance two-circle diffractometer (θ-2θ Bragg-Brentano mode) using Cu Kα radiation (λ = 1.54056 Å) equipped with a Ge(111) monochromator and a Lynx Eye detector. The analysis of the diffraction patterns was

performed by profile refinement using the FullProf and WinPlotr software packages[S4]. The XRPD data analysis of the raw sample indicates the coexistence of the $K_4Ta_6Br_{18}$ compound ($K_4Nb_6Cl_{18}$-type[S5], space group *C*2/*m*, a = 10.50(1) Å, b = 17.17(1) Å, c = 9.97(1) Å, β = 115.1(1)°, V = 1628.5(3) $Å^3$) as main phase with KBr and Ta as secondary phases.As described in the experimental section of the main article, these impurities were removed by dissolution by dissolution in ethanol and filtration.

XRD patterns of the functional surfaces were recorded by grazing incidenceX-ray diffraction (GIXRD), to limit the substrate contribution,using a RigakuSmartLab apparatus (Rigaku,Tokyo, Japan) equipped with a D/TeX Ultra 250 detector and Cu radiation in the θ–θ configuration.Data were collected in the 10–90° 2θ rangewith a step of 0.02° and a speed of $1°min^{-1}$.The XRD patterns consist of twobroad bands at 10.5 and 22°, attributed to the amorphousPVP.[S6] Indeed, in the figure S8 no diffraction peaks from Ta_6 clusters could be identified in both films deposited by dip-coating or spin-coating respectively. Diffraction peaks observed in thin Ta_6@PVP film came from ITO@glass substrate. These XRD results confirmed the good dispersion of Ta_6clusters in the PVP matrix, which was already demonstrated by UV-Vis results.

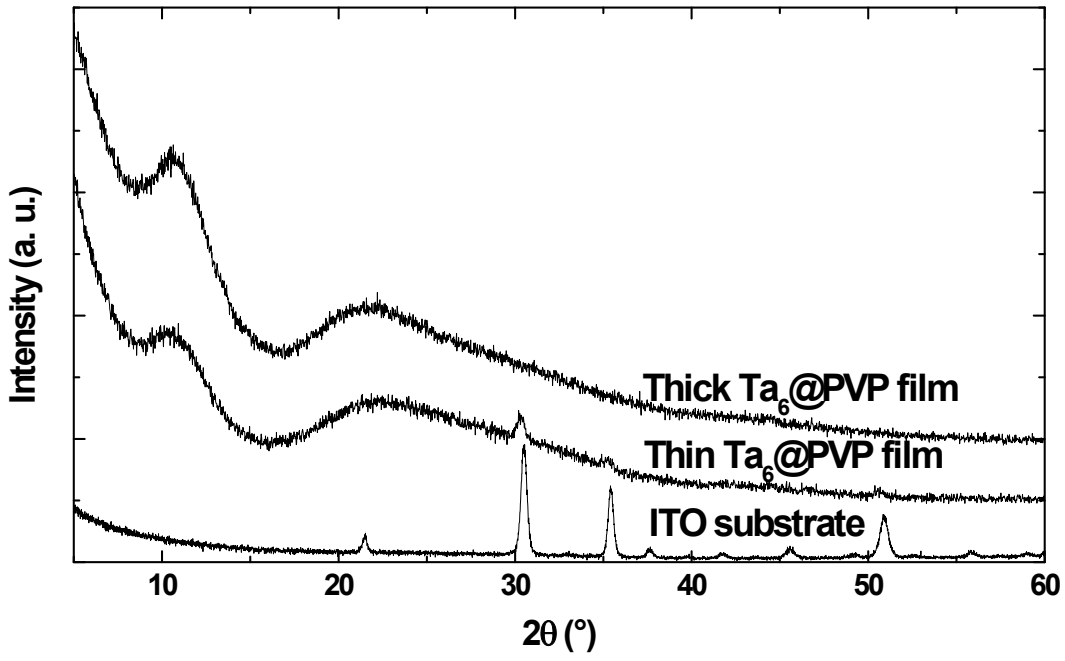

Fig. S8. XRD patterns of thick and thinTa_6@PVP films deposited by dip- and spin-coating respectively and compared with that of ITO substrate.

SEMimage.FE-SEM images were performed with a JEOL JSM 6301F microscope operating at 7 kV. STEM images were performed using a Hitachi SU8000 microscope operating at 30 kV.

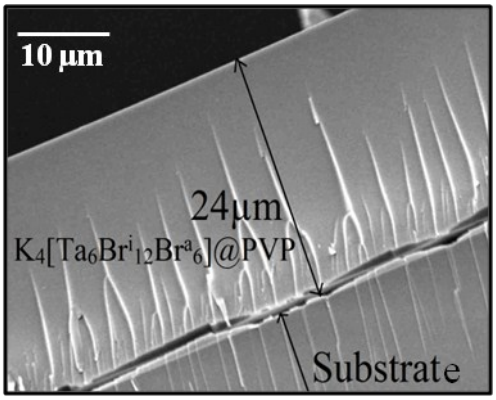

Fig. S9. FE-SEM image of the cross section of Ta_6@PVP@ITOfilm.

Electrochemical experiments. Cyclic voltammetry I-E curves were obtained with a three-electrodes(a working electrode in glassy carbon, a counter electrode in platinum and a reference in Ag/AgCl, Figure S10a) or a two (working electrode in ITO@glass and a counter-electrode/reference in Pt@ITO@glass, Figure S10b)electrochemical.

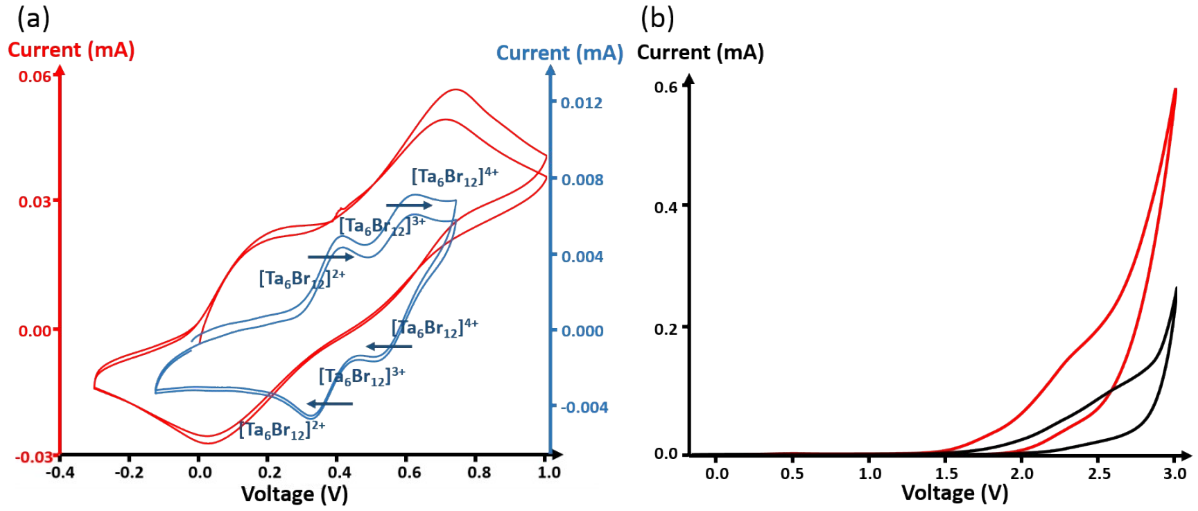

Fig. S10. (a) Cyclic voltammetry I-E curves of a Ta_6 cluster solution (0.7 mM of $K_4Ta_6Br_{18}$ in 0.1 mM $LiClO_4$ aqueous solution) obtained with a three-electrodes electrochemical circuit (i. e. a working electrode in glassy carbon, a counter electrode in platinum and a reference in Ag/AgCl) in blue and with a two-electrodes circuit corresponding to the electrochemical cell (namely a working electrode in ITO@glass and a counter-electrode/reference in Pt@ITO@glass) in red. (b) Cyclic voltammetry I-E curves of the same Ta_6 cluster solution (in red) and of the supporting electrolyte (0.1 mM $LiClO_4$ aqueous solution) carried out using the

two-electrodes electrochemical circuit. It clearly shows that the behaviour of I-E curves between 1.5 and 3 V is due to the solvent oxidation.

Calculation of color coordinates and FOM values. For proper comparison between the prepared samples and existing materials, we calculated the color coordinates (x, y, z) thanks to the procedure defined by the International Commission on Illumination (CIE 1931). Thus, we used the CIE standard illuminant D65, corresponding roughly to the average midday light in Western Europe / Northern Europe and the standard colorimetric observer for the 10° field obtained from the combined measurements of Stiles and Speranskaya.[S7]

The spectral transmittance spectrum of the sample T(λ) is multiplied by the spectral power distribution of an reference illuminant I(λ) giving the following equations:[S8]

$$X = \frac{1}{N}\int \bar{x}(\lambda) \times T(\lambda) \times I(\lambda)\, d\lambda \qquad \text{Eq. S1}$$

$$Y = \frac{1}{N}\int \bar{y}(\lambda) \times T(\lambda) \times I(\lambda)\, d\lambda \qquad \text{Eq. S2}$$

$$Z = \frac{1}{N}\int \bar{z}(\lambda) \times T(\lambda) \times I(\lambda)\, d\lambda \qquad \text{Eq. S3}$$

$$N = \int \bar{y}(\lambda) \times I(\lambda)\, d\lambda \qquad \text{Eq. S4}$$

Where $\bar{x}, \bar{y}$ and $\bar{z}$ are the CIE standard observer functions (10 degree). The integrals are computed over the visible spectrum (from 360 nm to 830 nm). We used the common reference D65. In practice, the functions found in these integrals exist either from empirical experiment or by measurement. Therefore, there are not mathematical equations representing them. Instead, they exist as discrete samples and so the integrals are replaced by summations:

$$X = \frac{1}{N}\sum_i \bar{x}i \times Si \times I \qquad \text{Eq. S5}$$

$$Y = \frac{1}{N}\sum_i \bar{y}i \times Si \times Ii \qquad \text{Eq. S6}$$

$$Z = \frac{1}{N}\sum_i \bar{z}i \times Si \times Ii \qquad \text{Eq. S7}$$

$$N = \sum_i \bar{y}i \times Ii \qquad \text{Eq. S8}$$

Then, given an XYZ colour whose components are in the nominal range [0,1]:

$$x = \frac{X}{X + Y + Z} \qquad \text{Eq. S9}$$

$$y = \frac{Y}{X + Y + Z} \quad \text{Eq. S10}$$

$$z = \frac{Z}{X + Y + Z} \quad \text{Eq. S11}$$

Moreover, the efficiency as saving energy of the prepared Ta_6-based UV and NIR filters was estimated *via* the determination of the different figure of merit (FOM) values such T_{vis}, T_{sol}, T_{vis}/T_{sol}.The solar transmittance T_{sol} is the integrated spectral transmittance of a window weighted with the normalized solar energy distribution spectrum. The visible transmittance T_{vis} is calculated in a similar way, but the solar transmittance is now weighted with the photopic response of the human eye. For more reliability, we include the equation leading to our figure of merit (FOM) values. T_{vis} and T_{sol} can be calculated by the following formula:[S9]

$$Tvis = \frac{\int_{300}^{1200} T(\lambda) \times X(\lambda)\, d\lambda}{\int_{300}^{2500} X(\lambda)\, d\lambda} \quad \text{Eq. S12}$$

$$Tsol = \frac{\int_{300}^{2500} T(\lambda) \times X(\lambda)\, d\lambda}{\int_{300}^{2500} X(\lambda)\, d\lambda} \quad \text{Eq. S13}$$

where T is the transmission spectrum as measured and X represents the Air Mass 1.5 (AM 1.5), which is equivalent to the spectrum of solar radiation after passing through 1.5 times the perpendicular atmospheric thickness in T_{sol}, or the human eye spectral response in T_{vis}. The CIE Colorimetric System (the CIE 1931 with 10° Standard Observer from 1964 and D65 source) was used for color analysis.

For the same reason as above, integrals were replaced by summations giving the following equations:

$$Tsol, Tvis = \frac{\sum_i Ti \times X}{\sum_i Xi} \quad \text{Eq. S14}$$

[S1] a) S. A. Best, R. A. Walton, *Inorg. Chem.* 1979,***18***,484; b) D. D. Klendworth, R. A. Walton, *Inorg. Chem.* 1981, ***20***, 1151.

[S2] H. El-Sayed, S. Singh, M. T. Greiner, P. Kruse, *Nano Lett.* 2006, ***6***, 2995.

[S3] K. Harder, W. Preetz, *Z. anorg. allg. Chem.*1990, ***591***, 32.

[S4] a) J. Rodriguez-Carvajal, Physica,1993,***B 192***, 55. b) T. Roisnel, J. Rodriguez-Carvajal, Mater. Sci. Forum, 2001, *118*, 378-381.

[S5] A. Simon, H.G. von Schnering, H. Schäfer, Z. Anorg. Allg. Chem. 1968,***361***,235.

[S6] T. G. Truong, B.Dierre, F.Grasset, N. Saito, N. Saito, T. K. N. Nguyen, K. Takahashi, T.Uchikoshi, M.Amela-Cortes, Y.Molard, S.Cordier, N.Ohashi, *Science and Technology of Advanced Materials*,National Institute for Materials Science, 2016,***17***, 443.

[S7] a) W. S. Stiles, J. M. Burch, *OpticaActa*1959, ***6***, 1; b) N. I. Speranskaya, *Opt. Spectroscopy,* 1959, **7**, 424; c) D. B. Judd, *in Proc.CIE Symposium on Advanced Colorimetry*, CIE Central Bureau, Vienna, Austria, 1993, pp. 107 – 114 ; d) P. W. Trezona, *Color Research and Application,*2001, **26**, 1.

[S8] B. J. Lindbloom, Site gathered the useful color information, http://www.Brucelindbloom.com, accessed: February, 2017.

[S9] G. B. Smith, C. A. Deller, P. D. Swift, A. Gentle, P. D. Garrett, W. K. Fisher, *J. Nanopart. Res.,*2002, **4**, 157.